

Accepted Manuscript

Research paper

Synthesis, spectroscopic characterization, DFT and antibacterial studies of newly synthesized cobalt(II, III), nickel(II) and copper(II) complexes with Salicylaldehyde N(4)-antipyrinylthiosemicarbazone

Ayman K. El-Sawaf, Maged A. Azzam, Amr M. Abdou, El Hassane Anouar

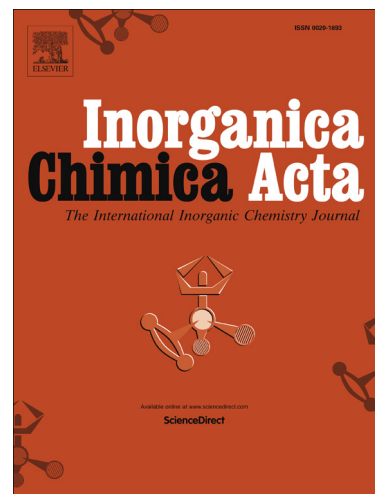
PII: S0020-1693(18)30824-7
DOI: <https://doi.org/10.1016/j.ica.2018.08.013>
Reference: ICA 18413

To appear in: *Inorganica Chimica Acta*

Received Date: 28 May 2018
Revised Date: 11 August 2018
Accepted Date: 12 August 2018

Please cite this article as: A.K. El-Sawaf, M.A. Azzam, A.M. Abdou, E.H. Anouar, Synthesis, spectroscopic characterization, DFT and antibacterial studies of newly synthesized cobalt(II, III), nickel(II) and copper(II) complexes with Salicylaldehyde N(4)-antipyrinylthiosemicarbazone, *Inorganica Chimica Acta* (2018), doi: <https://doi.org/10.1016/j.ica.2018.08.013>

This is a PDF file of an unedited manuscript that has been accepted for publication. As a service to our customers we are providing this early version of the manuscript. The manuscript will undergo copyediting, typesetting, and review of the resulting proof before it is published in its final form. Please note that during the production process errors may be discovered which could affect the content, and all legal disclaimers that apply to the journal pertain.



Synthesis, spectroscopic characterization, DFT and antibacterial studies of newly synthesized cobalt(II, III), nickel(II) and copper(II) complexes with Salicylaldehyde N(4)-antipyrinylthiosemicarbazone

Ayman K. El-Sawaf,^{a,b,*} Maged A. Azzam,^{a,b} Amr M. Abdou,^c El Hassane Anouar^{b,*}

^a Department of Chemistry, Faculty of Science, Menoufia university, Shebin El-Kom, Egypt.

^b Department of Chemistry, College of Science and Humanities, Prince Sattam Bin Abdulaziz university, BP 830, Al Kharj, Saudi Arabia.

^c Department of Microbiology and Immunology, National Research Centre 12622 Dokki, Giza, Egypt.

Corresponding author

Dr. Ayman K. El-Sawaf

E-mail: elsawaf2008@yahoo.com

Dr. El Hassane Anouar

E-mail: anouarelhassane@yahoo.fr

Abstract

Salicylaldehyde N(4)-antipyrinylthiosemicarbazone (H_2L) and its complexes of Co(III, II), Ni(II) and Cu(II) have been prepared and characterized. Elemental analyses, molar conductivities, magnetic measurements, spectral (IR, UV-vis, 1H and ^{13}C NMR and ESR) and thermogravimetric studies have been used to characterize the complexes. The infrared spectra show that the thiosemicarbazone ligand behaves as tridentate ligand (ONS), either in the thione or thiolato form. Stereochemistries are proposed for the complexes on the basis of both spectral and magnetic properties. Along with the experimental spectral data of the starting ligand, its corresponding predicted ones were obtained using the state of art density functional theory (DFT) in gas and solvent phases. The obtained results showed a relatively good correlation between the calculated and experimental spectral data. Some of the complexes showed antibacterial activity against *Staphylococcus aureus* and *Escherichia coli* representing Gram-positive and Gram-negative bacteria respectively when compared with Enrofloxacin as a standard antibiotic.

Keywords: Salicylaldehyde N(4)-antipyrinylthiosemicarbazone; complexes; spectral methods; thermal studies; DFT; antibacterial activity.

1. Introduction

The chemistry of thiosemicarbazones has conventional extensive attention because of their variable bonding manners, structural variety, ion-sensing capability [1, 2]. They are also known by their various biological implications such as antibacterial, antimalarial, antiviral and antitumor activities [3-5]. Thiosemicarbazones generally act as chelating agents with transition and non-transition metal ions tie through sulfur and nitrogen atoms, although in rare cases they behave as unidentate ligand with sulfur as the binding atom [6]. It was established that the dibasic tridentate thiosemicarbazones with ONS donor atoms are of enormous importance as they have a extensive variety of medicinal properties and can also offer dimetallic or polymeric species with uncommon structural and magnetic properties [7]. Great work is done on the biological activities of metal complexes of thiosemicarbazones [8-10]. The biological action of thiosemicarbazones is related to its chelating capability with metal ions, connecting through nitrogen, nitrogen and sulfur or oxygen, nitrogen and sulfur [11-13]. Previously, we have reported on the iron(III), cobalt(II, III), nickel(II), copper(II) and zinc(II) complexes of N(4)-antipyrinylthiosemicarbazone of 4-formylantipyrine and 2-formylpyridine [14, 15]. Recently, we have synthesized, characterized and investigated *in vitro* antibacterial activities of some Schiff base metal complexes[16]. Many metal complexes have potent antimicrobial activities and are already in common day-to-day use in medical field [17].

In the present paper, we report the synthesis, characterization and investigation of antibacterial activity of cobalt(II,III), nickel(II) and copper(II) complexes with salicylaldehyde N(4)-antipyrinylthiosemicarbazone (H_2L). Furthermore, DFT and TD-DFT calculations have been carried out in gas and polarizable continuum model phases at the B3LYP/LANL2DZ level of theory to predict the electronic and optical properties of the starting material salicylaldehyde N(4)-antipyrinylthiosemicarbazone.

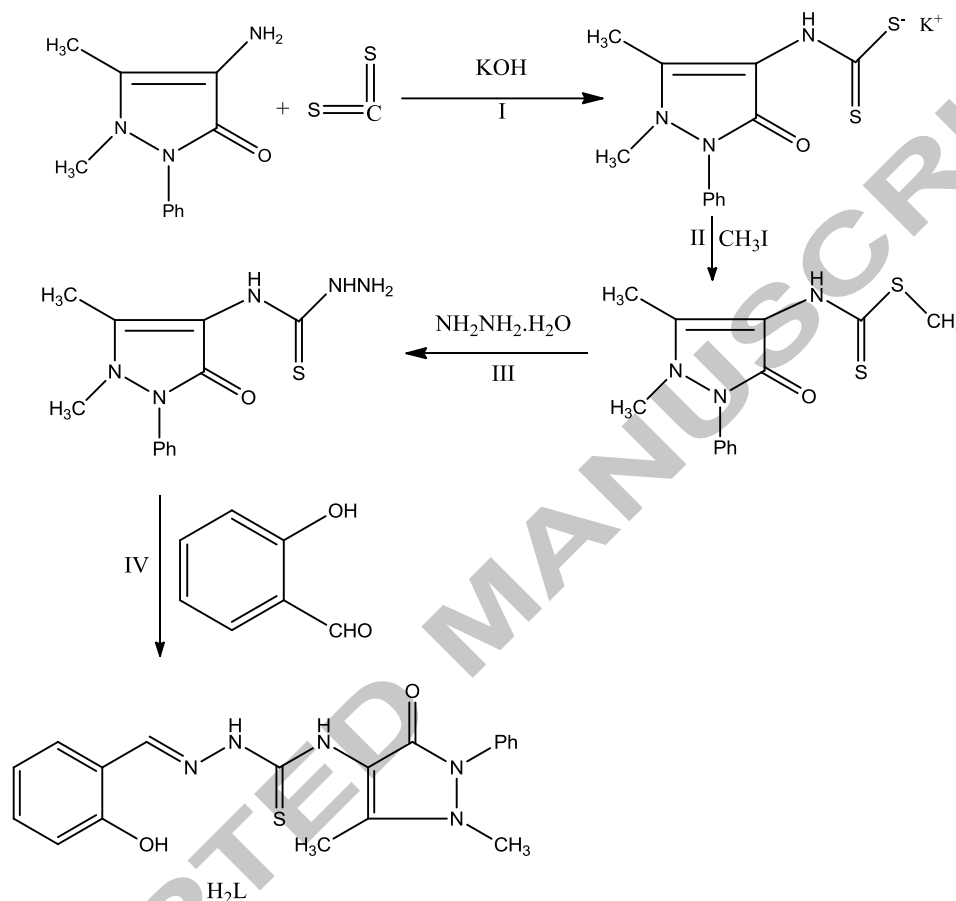
2. Materials and methods

2.1. Reagents and instruments

All reagents and solvents were used as obtained from the suppliers or recrystallized as necessary. Infrared spectra were recorded on a Nicolet FT-IR spectrophotometer in the range 4000-400 cm^{-1} . The ^1H and ^{13}C NMR spectra were recorded in $\text{DMSO-}d^6$ by using tetramethylsilane (TMS) as the internal solvent on a Bruker-400 MHz instrument. The electron paramagnetic resonance (EPR) spectra were recorded on a Varian E-109c spectrometer equipped with a field modulation unit at 100 kHz. Measurements were effected in the X-band on a microcrystalline powder at room temperature; the microwave power was around 10 mW. A Varian Cary 5000 spectrophotometer was used to perform the absorption electronic spectra as polycrystalline solid samples. Nujol mull electronic spectra were recorded on Whatman No.1 filter paper and referenced against another filter paper saturated in mineral oil. **The electronic spectra of dimethylsulfoxide solutions of both the thiosemicarbazone ligand and its metal complexes were recorded in 1 cm quartz cells and molar absorptivities were calculated using Beer's law.** Molar conductivity measurements were made in DMF solution 10^{-3} M using a type CD6N Tacussel conductimeter. The thermal analysis (TG) was carried out by using a Shimadzu DAT/TG-50 thermal analyzer with a heating rate of $10^\circ\text{C}/\text{min}$ under N_2 atmosphere from the room temperature up to 1000°C using platinum crucibles. Magnetic susceptibilities were measured at room temperature by a modified Gouy method by using a Johnson Matthey magnetic susceptibility balance. Diamagnetic corrections were calculated using Pascal's constants. The effective magnetic moments were calculated from the equation $\mu_{\text{eff}} = 2.84(X_{\text{M}}^{\text{corr}} T)^{1/2}$. Melting points were measured by using Stuart melting point apparatus. Biochemical measurements were carried out at The Department of Parasitology and Animal Diseases, National Research Center, Dokki, Egypt.

2.2. Synthesis of salicylaldehyde N(4)-antipyrinylthiosemicarbazone (H_2L)

The synthesis of N(4)-antipyrinylthiosemicarbazide was carried out in three steps (Scheme 1), as previously reported [14].



Scheme 1. Synthesis steps of salicylaldehyde N(4)-antipyrinylthiosemicarbazone ligand (H_2L).

The new Schiff base salicylaldehyde N(4)-antipyrinylthiosemicarbazone (H_2L) was prepared (step IV) by condensing N(4)-antipyrinylthiosemicarbazide with salicylaldehyde in the presence of few drops of H_2SO_4 to form a yellow product (Yield= 85% and m.p. 152 °C).

2.3. Synthesis of the metal complexes with H_2L

The metal complexes were prepared as follows: a solution of appropriate metal salt (3.15 mmol) in EtOH (30 cm^3) was mixed with a solution of the organic ligand (1.2g, 3.15 mmol) in EtOH (50 cm^3) and the mixture was stirred under reflux for 2 hours. The resulting solids were

filtered, washed with anhydrous diethyl ether and placed on a warm plate (35°C) until required for characterization.

2.4. Theoretical calculations

Geometry optimization and frequency calculations of the stable conformers of salicylaldehyde N(4)-antipyrinylthiosemicarbazone (H₂L) have been performed using DFT method at the B3LYP/LanL2DZ level of theory [18]. The calculated vibrational modes were scaled by a factor of 0.9679 [19]. The maximum electronic absorption bands, vertical electronic excitations and oscillator strengths ($f > 0$ for allowed transition) of the ligand salicylaldehyde N(4)-antipyrinylthiosemicarbazone was calculated using TD-DFT method at the same level of theory [20, 21]. NMR magnetic isotropic shielding tensors (σ) were predicted using the GIAO approach (Gauge-Independent Atomic Orbital) [22], using the above mentioned hybrid functionals. The isotropic shielding values were used to calculate the isotropic chemical shifts δ with respect to tetramethylsilane (Si(CH₃)₄). $\delta_{\text{iso}}(\text{X}) = \sigma_{\text{TMS}}(\text{X}) - \sigma_{\text{iso}}(\text{X})$, where δ_{iso} is isotropic chemical shift and σ_{iso} isotropic shielding constant. The predicted chemical shifts were obtained using the equation $\delta_{\text{exp}} = a\delta_{\text{cal}} + b$, where $\delta_{\text{cal}} = \delta_{\text{iso}}$. The theoretical calculation in solvent were obtained using polarisable continuum model (PCM), in which the solute is embedded into a cavity surrounded by a dielectric continuum solvent described by its dielectric constant (e.g., $\epsilon_{\text{CDCl}_3} = 4.7113$) [23]. The PCM has been reported to correctly model major solvent effects such as electrostatic effects of the medium providing no specific solute-solvent interactions such as hydrogen bond interactions, dipole-dipole interactions, or induced dipole-dipole interactions are considered [24]. Theoretical calculations were performed using Gaussian09 package [25].

2.5. Screening for the antibacterial activity

The bacterial cultures used in this study were *Staphylococcus aureus* as representative for Gram-positive bacteria and *Escherichia coli* as representative for Gram-negative bacteria. The test organisms were kindly provided by The Department of Parasitology and Animal Diseases, National Research Center, Dokki, Egypt. The test organisms were maintained on agar slant at 4 °C and subcultured on a fresh agar plates. For disc diffusion assay, bacterial liquid cultures were initiated by placing a loop of bacteria from the slant into 10 ml of lysogeny broth (LB) media. Agar diffusion test was conducted to detect the bacterial susceptibility to the prepared compounds [26]. A volume of 100 µL of cell culture suspension matching with 0.5 Mc-Farland of each test organism were spread onto the surface of solid agar medium (Muller Hinton agar). The prepared compounds were adjusted to a concentration of 50 mg/mL using DMSO as solvent. Filter paper discs with a diameter of 7 mm each were impregnated with 15 µL of each of the different compounds. Then the agar plates containing microorganisms, soaked with paper discs (5 µg) were incubated at 37 ± 0.1 °C for 24 h. The inhibition of bacterial growth was evaluated by measuring the diameter (cm) of the clear zone around each disc. Enrofloxacin antibiotic discs were used as positive control. Filter paper discs impregnated with 15 µL of DMSO were also used as control for the solvent.

3. Results and discussion

3.1. Elementary analyses

The stoichiometries of the salicylaldehyde N(4)-antipyrinylthiosemicarbazone (H_2L) and its complexes are shown Table 1. Complexes of the monobasic ligand (*i.e.*, loss of OH proton) are formed with the chlorides of cobalt(II) and nickel(II), cobalt(II) nitrate, Cu(II) acetate and Cu(II) perchlorate. Complexes of the dibasic ligand (*i.e.*, loss of OH and N(2)H protons) are formed on complexation with cobalt(II) acetate. In addition $[Co(HL)(L)]$ was isolated with a combination of mono and dibasic ligands. All complexes obtained are stable to air and moisture and are

appreciably soluble in DMF and DMSO. The colors, partial elemental analysis, molar conductivities and magnetic susceptibilities of the metal complexes are shown in Table 1. The green, brown, red and blue colors are common to complexes involving thiosmeicarbazone coordination owing to the sulfur to metal charge transfer bands, which dictate their visible spectra [27]. The values of Λ_m showed in Table 1, indicated that all the metal complexes have conductivity values lie in the range characteristics for the non-electrolytic performance of these complexes due to lack of counter ions in the suggested structures of these complexes [28]. The fairly higher values detected for the chloro complexes may due to partial decomposition of these complexes in solution with the DMF solvent molecules relocating the halo ligands [15].

Table 1

Colors, partial elemental analyses, molar conductivities and magnetic susceptibilities of the metal complexes of salicylaldehyde N(4)-antipyrinylthiosemicarbazone.

No	Chemical formula	F.W. Color	M. p. (°C)	Found (Calcd. %)					Λ_M^a	$\mu(\text{B.M.})$
				C	H	N	M	Cl		
H₂L	C ₁₉ H ₁₉ N ₅ O ₂ S	381.461 Pale yellow	152	60.21 (59.82)	4.97 (5.02)	18.18 (18.36)	- -	- -	-	-
1	[Co(HL)(L)] C ₁₉ H ₂₉ N ₅ O ₈ SCo	818.828 Dark brown	198	55.23 (55.74)	4.62 (4.31)	17.62 (17.11)	7.32 (7.20)	-	9.3	0.0
2	[Co(L)(H ₂ O)].5H ₂ O C ₁₉ H ₂₉ N ₅ O ₈ SCo	546.501 Brown	142	41.88 (41.76)	4.73 (5.35)	12.38 (12.82)	10.07 (10.78)	-	10.4	1.97
3	[Co(HL) ₂].5H ₂ O.0.5EtOH C ₃₉ H ₄₉ N ₁₀ O _{9.5} S ₂ Co	932.95 Brown red	170	50.96 (50.21)	4.78 (5.29)	15.63 (15.01)	6.53 (6.32)	-	8.7	4.82
4	[Ni(HL)Cl].2.5H ₂ O. 0.25 EtOH C _{19.5} H _{24.5} N ₅ O _{4.75} SNiCl	531.15 Yellow	210	44.87 (44.09)	5.01 (4.65)	13.31 (13.19)	10.85 (11.05)	6.85 (6.67)	11.7	2.21
5	[Ni(L)H ₂ O].3.5H ₂ O C ₁₉ H ₂₆ N ₅ O _{6.5} SNi	519.207 Buff	175	43.46 (43.95)	4.88 (5.05)	13.67 (13.49)	11.21 (11.30)	-	10.9	0.0
6	[Cu(HL)Cl].3.75H ₂ O C ₁₉ H _{25.5} N ₅ O _{5.75} SCuCl	547.012 Dark brown	240	42.24 (41.72)	3.72 (4.66)	12.87 (12.80)	11.83 (11.17)	6.34 (6.48)	14.3	1.78
7	[Cu(HL)(CH ₃ COO)].2.25H ₂ O C ₂₁ H _{25.5} N ₅ O _{6.25} SCu	543.581 Dark brown	205	46.27 (46.40)	4.89 (4.73)	13.79 (12.88)	11.35 (11.69)	-	12.7	1.70
8	[Cu(HL)(ClO ₄)].0.5H ₂ O. 0. 5 EtOH C ₂₀ H ₂₂ N ₅ O ₇ SCuCl	575.495 Green	-	42.08 (41.74)	4.11 (3.85)	11.89 (12.17)	11.67 (11.04)	-	12.4	1.73

^a10⁻³M in DMF and expressed as $\Omega^{-1} \text{ cm}^2 \text{ mol}^{-1}$

3.2. ^1H and ^{13}C NMR spectra

To get an insight into the demonstrated ligand structure (H_2L , Fig. 1), its calculated and experimental ^1H and ^{13}C NMR chemical shifts in $\text{DMSO-}d^6$ have been carried out and approves its preparation (Table 2). The absence of a signal from thiol $-\text{SH}$ (Fig. 2) which would be expected around 4 ppm,[29] strongly confirms the presence of the ligand thione form. The spectrum shows the phenolic OH proton at δ (p.p.m.) = 11.83 (s, 1H, O-H), suggesting intramolecular hydrogen bonding to N(1)[30] the N(2)H at δ (p.p.m.) = 9.95 (s, 1H, N(2)H), the N(4)H at δ (p.p.m.) = 9.32 (s, 1H, N(4)H). The spectrum also shows the formyl proton, $\text{CH}=\text{N}$ at δ (p.p.m.) = 8.48 (s, 1H, C-H). The other resonances in the spectrum of the ligand are at δ (p.p.m.) = 7.34-7.23 (m, 5H) corresponding to the phenyl protons, δ (p.p.m.) = 3.40 (s, 3H, N- CH_3) and δ (p.p.m.) = 2.51 (s, 3H, C- CH_3) corresponding to N- CH_3 and C- CH_3 of the antipyrinyl moiety, respectively. Signals for aromatic protons are found as multiplets in the 8.08-6.83 ppm range[31]. Somehow, the experimental ^1H NMR chemical shifts are well produced, mainly those bonded to carbon atom. For instance, the experimental and calculated chemical shifts of H8 are 8.47 and 8.48 ppm, respectively. The ^{13}C NMR spectrum exposed the presence of anticipated number of signals related to different types of carbon atoms present in the compounds (Table 1 and Fig. 3). The signals observed at 178.55 and 162.85 ppm are due to $\text{C}=\text{S}$ and $\text{C}=\text{O}$ of the pyrazolone ring, respectively. The spectrum of the ligand shows a strong signal at δ 157.03 ppm due to $\text{C}=\text{N}$ group. Similarly, the calculated ^{13}C chemical shift are relatively in agreement with the observed ones. For instance, a variation of about 0.51 ppm is obtained between the experimental and calculated chemical shifts of C8 (Table 2).

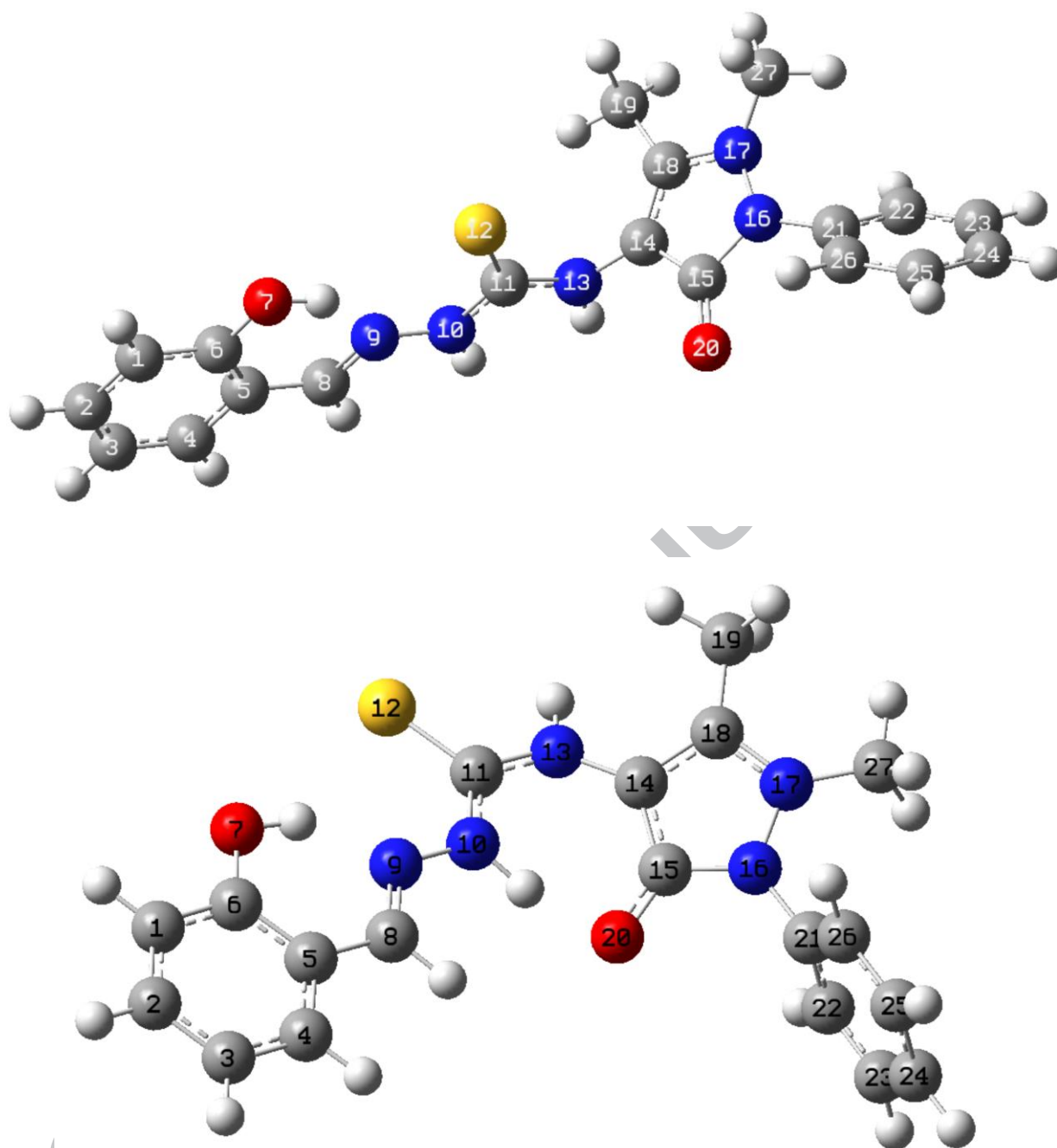


Fig. 1. The optimized structures of the stable conformers of ligand (H_2L) obtained at the B3LYP/LANL2DZ level of theory.

Table 2

Calculated and experimental ^1H and ^{13}C NMR chemical shifts (ppm) of salicylaldehyde N(4)-antipyrinylthiosemicarbazone (H_2L) in $\text{DMSO-}d^6$.

	Calculated	Experimental
$^1\text{H-NMR}$		
H1	7.79	
H2	8.07	
H3	7.68	7.34-7.23
H4	7.88	
H7 (OH)	7.88	11.83
H8	8.47	8.48
H10 (NH)	8.19	9.95
H13 (NH)	5.94	9.32
H19	2.23	2.51
H22	7.61	
H23	8.21	
H24	8.16	8.08-6.83
H25	8.19	
H26	8.09	
H27	3.46	3.4
$^{13}\text{C-NMR}$		
C1	122.48	116.55
C2	137.02	110.28
C3	124.78	116.55
C4	137.83	120.78
C5	120.74	140.33
C6	165.76	129.56
C8	157.54	157.03
C11	199.22	178.55
C14	109.80	154.94
C15	169.20	162.85
C18	159.23	162.85
C19	15.54	140.33
C21	139.22	11.68
C22	129.19	135.79
C23	134.12	-
C24	132.20	129.56
C25	133.88	127.32
C26	132.50	126.57
C27	41.01	123.83

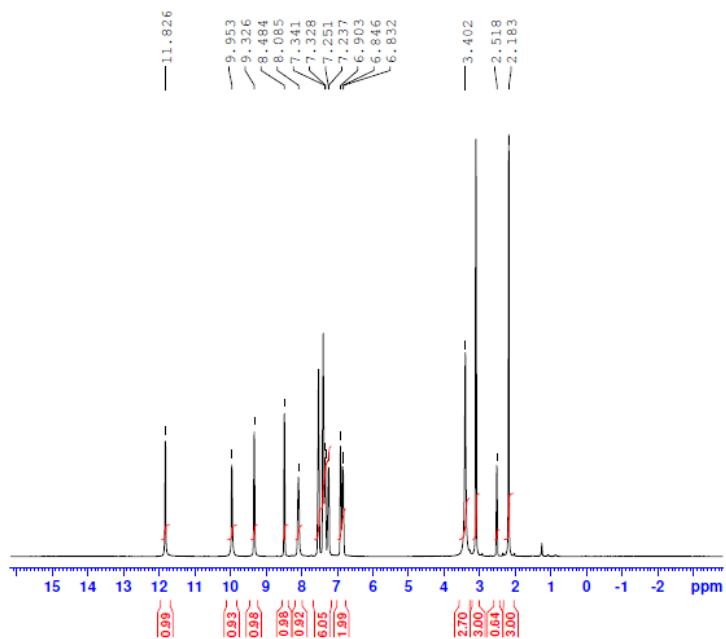


Fig. 2 ^1H NMR spectrum of the ligand H_2L

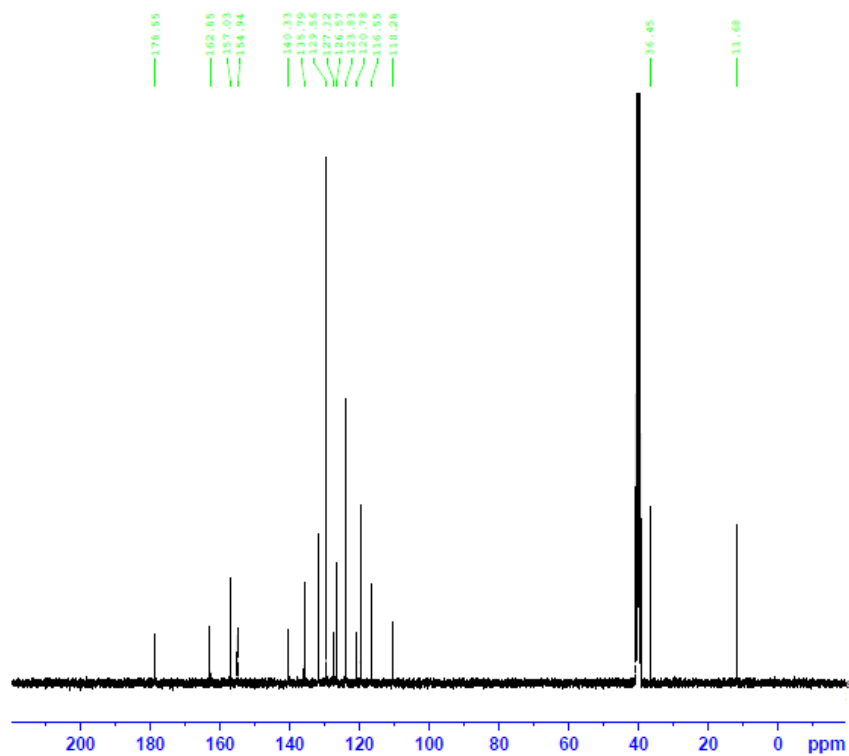


Fig. 3 ^{13}C NMR spectrum of the ligand H_2L

Consistent with its loss on complexation, the signals due to phenolic OH and N(2)H protons are absent in the ^1H NMR spectra of the Co(III), complex (1), and square planar Ni(II), complex (5), (Figs. S1 and S2). The spectra of these complexes features the N(4)H peak shifted slightly downfield compared to the free ligand because of coordination of the thiol sulfur resulting in reduced electron density at N(4) position [32] ($\delta = 9.32$ to 9.56 and 9.59 for complexes 1 and 5 respectively). Also, the formyl proton, CH=N, shifts downfield from $\delta = 8.48$ to 8.78 and 8.62 for complexes 1 and 5 respectively due to coordination of the azomethine nitrogen and indicating that the metal centers has drawn considerable electron density from the azomethine group as has been noticed previously [33].

3.3. Infrared spectra

The main experimental infrared spectral data of the free thiosemicarbazone ligand (H_2L) and its metal complexes with cobalt(II, III), nickel(II) and copper(II) are presented in Table 3 and shown in Fig. S3. The absence of any band in $2500\text{-}2000\text{ cm}^{-1}$ region which is due to $\nu(\text{S-H})$ in the spectra of the complexes indicates that the ligand exists mainly in the thione form[34]. It has been recognized that the salicylaldehyde thiosemicarbazone of complexes 2, 4, 6, 7 and 8 act as monodeprotonated tridentate ligand and are coordinated to the central ions via deprotonated phenolic oxygen, azomethinic nitrogen and sulfur atom creating five and six membered metalocycles [12, 35]. The spectrum of the free ligand shows a broad band at 3430 cm^{-1} related to phenolic group $\nu(\text{OH})$. This band disappeared from the IR spectra of all complexes. Additionally, this is confirmed by the shift of $\nu(\text{C-O})$ stretching vibration bands observed in the range of $1210\text{-}1150\text{ cm}^{-1}$ in the spectra of the complexes. This is further confirmed by the presence of the band looking in the region $490\text{-}450\text{ cm}^{-1}$ assigned to the $\nu(\text{M-O})$ frequency [36]. The medium intensity band at 1610 cm^{-1} in the spectrum of the free ligand has been assigned to $\nu[(\text{C}(7)=\text{N}(1))]$. Its corresponding scaled value obtained at B3LYP level of theory is appeared at 1589 cm^{-1} with a variation of 21 cm^{-1} to the experimental value. This band shifts to lower wavenumbers by $5\text{-}15\text{ cm}^{-1}$ in the spectra of the complexes, indicating bonding to the azomethine nitrogen in coordination [37]. In addition, the $\nu(\text{C=N})$ mode may be joined with $\nu(\text{C=S})$ to give the intense band detected at

1360 cm^{-1} [38], and the lower frequency shift of this band in the spectra of the complexes supports coordination of the azomethine nitrogen. The band at 950 cm^{-1} in the spectrum of H_2L attributed to $\nu(\text{N-N})$ endures a positive shift in all complexes which is owing to the increase in double bond character off-setting the loss of electron density through donation to the metal ion. This confirms the coordination of the azomethine nitrogen to the metal ions [39]. The appearance of a $\nu(\text{M-N})$ band at 530-485 cm^{-1} provides further support for the nitrogen donor [40]. The band at 1360 cm^{-1} in the H_2L spectrum, which has $\nu(\text{C=S})$ character, disappears in the spectrum of complex **5**, $[\text{Ni}(\text{L})\text{H}_2\text{O}]$, due to the alteration in the nature of NH-C(=S)-N to N=C(-S)-N on complexation[41]. The high intensity band at 860 cm^{-1} in the spectrum of the thiosemicarbazone ligand, due to the thioamide IV band, which has a substantial contribution from $\nu(\text{CS})$, shifts to *ca.* 800 cm^{-1} for complexes with the monobasic ligand and at 755 cm^{-1} for the dibasic ligand, representing coordination of the thione/thiolato sulfur atom [42]. As is expected, larger decreases in the thioamide IV band occur for dibasic form of the ligand due to C-S formally becoming a single bond[43]. In addition, a band at *ca.* 420 cm^{-1} is due to $\nu(\text{MS})$, which approves coordination of the thione/thiolato sulfur [44]. The presence of the water molecule in the coordination sphere of complexes **2** and **5** is reinforced by the occurrence of bands at *ca.* 3600, *ca.* 1580, 980 and *ca.* 630 cm^{-1} owing to $\nu(\text{OH})$, $\delta(\text{H}_2\text{O})$, $\rho_{\text{rock}}(\text{H}_2\text{O})$ and $\rho_{\text{wagg}}(\text{H}_2\text{O})$, respectively [45]. The last two modes are absent from the spectra of the rest of the isolated complexes with water molecules, representing hydrate rather than coordinated water [46]. The acetato group in complex (7) acts as a unidentate ligand based on the appearance of two new bands at 1610 and 1330 cm^{-1} , which are assignable to $\nu_{\text{a}}(\text{CO}_2)$ and $\nu_{\text{s}}(\text{CO}_2)$, respectively [47]. Further, the complex exhibits $\delta(\text{COO})$ at 760 cm^{-1} , which is considered indicative for unidentate acetate ligands[48]. The spectrum of the perchlorate complex, $[\text{Cu}(\text{HL})(\text{ClO}_4)]$, (Fig. 4) shows bands at 1107 (ν_3), 910 (ν_1), 630 (ν_4) and 490 (ν_2) cm^{-1} , suggesting the monodentate coordination of perchlorate ion to copper ion[49].

Table 3Selected IR band assignments of the ligand (H₂L) and its metal complexes.

No.	Ligand/complex	ν [N(2)H]	ν (C=N)	ν (C-O) phenolic	ν (N-N)	ν (C-S)	ν (M-N)	ν (M-O)	ν (M-S)
	H ₂ L	3190(br)	1610(m)	1250(s)	950(m)	860(m)	--	--	--
1	[Co(HL)(L)]	3110(s)	1600(m)	1170(m)	980(s)	760(m)	500(m)	485(sh)	435(w)
2	[Co(L)(H ₂ O)].0.5 H ₂ O	3135(s)	1602(m)	1175(w)	1000(s)	745(s)	485(m)	470(w)	420(s)
3	[Co(HL) ₂].5H ₂ O.0.5EtOH	3130(m)	1595(w)	1180(w)	959(m)	810(w)	515(m)	490(sh)	445(s)
4	[Ni(HL)Cl].2H ₂ O. 0.25 EtOH	3050(w)	1600(m)	1210(w)	950(s)	825(w)	495(w)	460(w)	435(w)
5	[Ni(L)H ₂ O].3.5H ₂ O	3135(m)	1600(w)	1180(m)	995(s)	755(s)	520(m)	465(s)	415(sh)
6	[Cu(HL)Cl].3.75H ₂ O	3110(w)	1604(s)	1150(w)	1035(w)	835(w)	530(m)	490(s)	405(w)
7	[Cu(HL)(CH ₃ COO)].2.25H ₂ O	3233(w)	1599(s)	1200(m)	1090(w)	850(w)	490(w)	450(w)	420(w)
8	[Cu(HL)(ClO ₄)].0.5H ₂ O. 0.5 EtOH	3220(w)	1605(w)	1205(m)	1105(s)	820(w)	490(s)	460(w)	435(w)

3.4. *Magnetic susceptibilities and Electronic spectra*

The electronic absorption spectra are frequently very helpful in the estimation of results provided by other methods of structural analysis. The tentative assignments of the major electronic spectral bands of ligand and its metal ion complexes in solid state are shown in Table 4. Omitted from Table 4 are the higher energy $\pi \rightarrow \pi^*$ transitions at *ca.* 37000 cm^{-1} (270 nm), of the free ligand H₂L, which are slightly shifted upon the complexation of free ligand with the tilted metals. The shift of the $\pi \rightarrow \pi^*$ bands to lower energy in complexes is the result of the C=S bond being faded and the conjugation system enhanced on complexation[50]. The $n \rightarrow \pi^*$ transition associated with the phenol function at 31710 cm^{-1} (315 nm) in the ligand spectrum generally shifts to higher energy by *ca.* 800 cm^{-1} (324 nm) in the spectra of the complexes [51]. The second $n \rightarrow \pi^*$ band, which appears at 29670 cm^{-1} (337 nm) in the uncomplexed thiosemicarbazone spectrum, merges with the first $n \rightarrow \pi^*$ band in the spectra of some of complexes (Fig. 4). The corresponding calculated λ_{max} (nm) of the second $n \rightarrow \pi^*$ (HOMO-1 \rightarrow LUMO) band for both stable conformers of the ligand H₂L in gas and solvent phases at the B3LYP/LANL2DZ level of theory are presented in Table 5. The results clearly show the strong effect of the solvent, which induces an hypsochromic shift of λ_{max} . This shift is mainly due to the solute-solvent interaction, which stabilizes the HOMO-1 and LUMO orbitals by 0.72 and 0.28 eV, respectively. The experimental λ_{max} is well produce with the chose methodology, with a variation less the 2 nm compared to the experimental value. The choice of methodology is in good settlement with our previous studies [52, 53]. The conformation has no strong effect of λ_{max} shift, which is less than 2 nm for the current conformers. This results is in accordance with our previous studies [54].

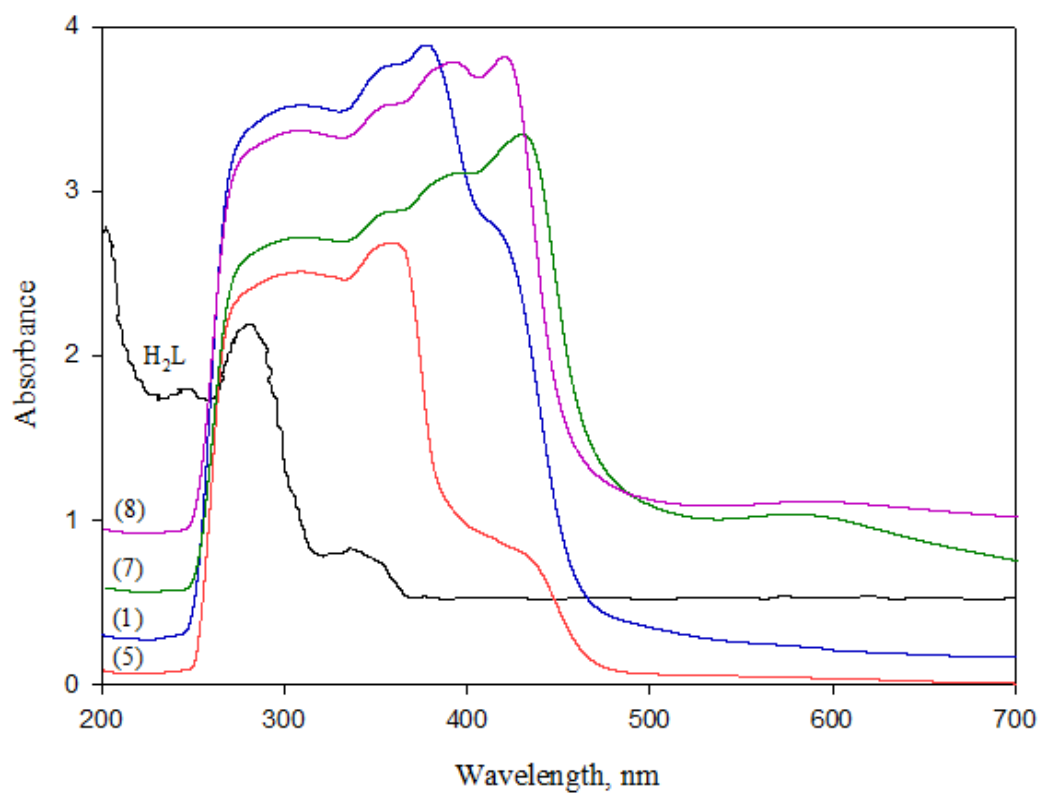


Fig. 4 Solid state Nujol mull electronic absorption spectra of **1**, **5**, **7** and **8** complexes.

Table 4 Solid state electronic spectra (cm^{-1}) of the ligand and its metal complexes

No.	Compound	Intraligand and charge transfer bands	d-d bands
	H ₂ L	31710, 29670	
1	[Co(HL)(L)]	32680, 28010, 24200, 20450	16830, 13470, 10990
2	[Co(L)(H ₂ O)].5H ₂ O	32570, 28490, 25770	18050, 10710
3	[Co(HL) ₂].5H ₂ O.0.5EtOH	32790, 28740, 26110, 23530	18920, 14710, 11420
4	[Ni(HL)Cl].2.5H ₂ O. 0.25 EtOH	32840, 28250, 25840, 23470	14490, 12000, 11420, 11010
5	[Ni(L)H ₂ O].3.5H ₂ O	32410, 28330, 26420, 22350	16720, 16200
6	[Cu(HL)Cl].3.75H ₂ O	32410, 28410, 25670, 24300	14340, 11010
7	[Cu(HL)(CH ₃ COO)].2.25H ₂ O	33330, 28330, 25740, 23280	11060
8	[Cu(HL)(ClO ₄)].0.5H ₂ O. 0. 5 EtOH	32950, 28330, 25710, 24450	16960, 11050

Table 5 Calculated λ_{max} (nm) of the stable conformers of the ligand H₂L in gas and solvent phases at the B3LYP/LANL2DZ level of theory.

	Calculated			Experimental	
	λ_{max} (cm^{-1})	λ_{max} (nm)	f	λ_{max} (cm^{-1})	λ_{max} (nm)
Gas					
Conf. 1	657474	353	0.36		
Conf. 1	28458	351	0.35		
				29670	337
IEF-PCM					
Conf. 1	29435	340	0.41		
Conf. 1	29586	338	0.39		

This band, which includes transitions inside the thiosemicarbazone moiety [mainly, C=N and C=S groups], is of reduced intensity and shifts to higher energy on complexation. Two ligand-to-metal charge transfer bands are found at 24000-27000 cm^{-1} and 21000-25000 cm^{-1} in the spectra of the metal complexes (Fig. 4). In agreement with studies of previous thiosemicarbazone complexes [55], the higher energy band is assigned to $S(\pi) \rightarrow M(\text{II, III})$ transitions [56]. The band in the 21000-25000 cm^{-1} range is related to phenoxy $O \rightarrow M(\text{II,III})$ transitions [57].

[Co(HL)(L)] is diamagnetic, $\mu_{\text{eff}} = 0$, confirming its oxidation to cobalt(III) during preparation, which commonly occurs with heterocyclic thiosemicarbazones [14]. Assuming O_h symmetry the assignments for the $d \rightarrow d$ bands are as follows: ${}^1A_{1g} \rightarrow {}^1T_{1g}(\nu_1)$ 20450 cm^{-1} , ${}^1A_{1g} \rightarrow {}^1T_{2g}(\nu_2)$ 24200 cm^{-1} , ${}^1A_{1g} \rightarrow {}^3T_{1g}(\nu_3)$ 6850 cm^{-1} and ${}^1A_{1g} \rightarrow {}^3T_{2g}(\nu_4)$ 16830 cm^{-1} . Calculations of the ligand field parameters give $D_q = 2016 \text{ cm}^{-1}$, $B = 741 \text{ cm}^{-1}$ and $\beta = 0.67$ [51]. The value of the nephelauxetic parameter, β , indicates the significant covalent character for the metal-ligand σ -bonds[55]. The brown [Co(L)(H₂O)].0.5H₂O complex shows a magnetic moment of 1.97 B.M. suggesting a square planar cobalt(II) species with spin-orbit coupling [56]. The electronic spectrum of this complex exhibits three bands at 9100, 9800 and 15820 cm^{-1} . The first and third bands may be assigned to ${}^2A_{1g} \rightarrow {}^2E_g$ and ${}^2A_{1g} \rightarrow {}^4E_g$ transitions, respectively, assuming square planar geometry around Co(II). The band at 9800 cm^{-1} is considered as characteristic band for Co(II) in a square planar environment [51]. This band may be taken as equal to 15 B from which B is calculated as 653.3 cm^{-1} . The calculated magnetic susceptibility for [Co(HL)₂].5H₂O.0.5EtOH is 4.82 B.M., which indicating a spin quartet cobalt(II) ground state and is in the range generally accepted for octahedral structures [57]. The electronic absorption spectrum of this complex exhibits three bands at 15620, 18470 and 20950 cm^{-1} . These bands are related to the transitions ${}^4T_{1g}(\text{F}) \rightarrow {}^4T_{2g}(\text{F})(\nu_1)$; ${}^4T_{1g}(\text{F}) \rightarrow {}^4A_{2g}(\text{F})(\nu_2)$ and ${}^4T_{1g}(\text{F}) \rightarrow {}^4T_{2g}(\text{P})(\nu_3)$ respectively suggesting an octahedral geometry [58].

The magnetic moment observed for the [Ni(HL)Cl].2H₂O. 0.25 EtOH complex is 3.58 B.M which is consistent with the tetrahedral stereochemistry of the complex [59] and the electronic spectrum of the complex shows two bands at 9740 cm⁻¹ and 14490 cm⁻¹ which may be assigned to ³T₁(F)→³A₂ (ν₂) and ³T₁(F)→³T₂ (P) (ν₃) transitions, respectively, for the tetrahedral nickel(II)[55]. The transition ³T₁(F)→³T₂ (ν₁) is expected to be in the range of 3000-5000 cm⁻¹ and the theoretical calculation of this band is 4460 cm⁻¹. The assigned energies were used to calculate the following spectral parameters for [Ni(HL)Cl].2H₂O. 0.25 EtOH: Dq = 520, B = 717 and β = 0.69. These values agree well with those reported for tetrahedral nickel(II) complexes [56].

At room temperature the, [Ni(L)H₂O].3.5H₂O, complex shows a diamagnetic performance which shows the square planar situation around Ni(II) ion [60, 61]. The spectrum of this diamagnetic complex shows a band at 22350 cm⁻¹ due to a combination of ¹A_{1g}→¹B_{1g} and S →Ni(II) transitions and bands at 18850 and 16570 cm⁻¹ attributable to the ¹A_{1g}→¹A_{2g} and ¹A_{1g}→¹E_g transitions, consistent with square-planar geometry around the nickel(II) ion [48, 62]. The room temperature magnetic moment of the solid copper (II) complexes **6**, **7** and **8** was found in the range 1.70–1.78 BM, revealing one unpaired electron per Cu(II) [63] and the two low intensity bands for copper(II) complexes are in the ranges 18600-17540 cm⁻¹ and 16240-14280 cm⁻¹ are consistent with d → d transitions of square planar copper(II) complexes [17].

The solution electronic (DMSO) maxima of H₂L and its metal complexes are presented in Table S1. The Schiff base ligand and its metal complexes exhibit three absorption peaks at lower energy region (< 40000 cm⁻¹). The stronger and higher energy peak (Fig. S4) at 38000 cm⁻¹ was attributed to the π→π* transitions of the azomethine chromophore and the phenyl ring and is nearly unshifted in the spectra of all complexes, while the weaker and less energetic peak at 29670 cm⁻¹ is owing to the n→π* transition associated with the thione portion of the thiosemicarbazone moiety. The band at 32750 cm⁻¹ (log ε = 4.21) in the spectrum of the organic ligand, H₂L, is assigned to the n→π* transition of the azomethine portion.

The solution spectra of the complexes exhibit an intense transition in the range 33760-3462 cm⁻¹ (log ε = 4.36-4.61) owing to a n→π* transition of the azomethine portion of the thiosemicarbazone.

Also, the band associated with the $n \rightarrow \pi^*$ transition of the thione portion of the thiosemicarbazone moiety is shifted to higher energy in the spectra of all complexes and sometimes merges with the $n \rightarrow \pi^*$ transition of the azomethine portion of the thiosemicarbazone. Bands in the 23240-25530 cm^{-1} range are due to $S \rightarrow \text{metal(II,III)}$ and other ligand to metal charge transfer bands [63]. The $d \rightarrow d$ spectra of the metal complexes show different energies in solution compared to the solid state indicating significant interactions with the DMSO solvent.

3.5. Thermal studies

The thermogravimetric data of the ligand and some of its metal complexes are given in Table 6 and represented in Fig. 5. The thermogram of the ligand reveals that no detectable weight loss within 25-155 °C range indicating that the ligand exhibits thermal stability up to 155 °C, which is compatible with its measured melting point (Table 6). Also, the absence of any residual solvent in the tested sample. After that the ligand starts its thermal decomposition through one well-defined step at temperature range 155-420 °C with weight loss 80.86% equivalent to removal of $\text{C}_{13}\text{H}_{19}\text{N}_5\text{O}_2\text{S}$. This stage is associated with a sharp DTG peak at $T_{\text{max.}}=255$ °C. Indicating that the ligand pyrolysis proceed fast in progressive nature [16]. The last stage involves a weight loss of 11.34% corresponding to complete ligand pyrolysis at temperature range 420-1000 °C. The complexes $[\text{Co}(\text{L})\text{H}_2\text{O}]\cdot 5\text{H}_2\text{O}$ (2) and $[\text{Ni}(\text{L})\text{H}_2\text{O}]\cdot 3.5\text{H}_2\text{O}$ (5) are isostructural and the TG data (Table 6) show similar thermal degradation patterns (isothermal behavior). The thermal behavior for complex (2) will be presented as a model example (Scheme 2). The TG curve displayed weight losses at temperature range 25-140 °C corresponding to removal of five molecules of water. The dehydration processes is followed by thermal decomposition stage associated with 40.02% TG weight loss at 140-350 °C range. This weight loss compatible with removal of $\text{C}_{11}\text{H}_{12}\text{N}_3\text{O}$ fragment and coordinated water molecule and characterized by DTG peaks at $T_{\text{max.}}=168$ and 248 °C respectively. The final pyrolysis step demonstrated by a broad DTG peak at 770 °C and by TG weight loss of 28.42% up to 1000 °C due to removal of $\text{C}_{7.75}\text{H}_5\text{N}_2\text{S}$ and leaving 14.20% of $\text{CoO}+0.25\text{C}$ as final residue. The proposed thermal degradation mechanism is shown in scheme 2. The TG curve of the octahedral $[\text{Co}(\text{HL})_2]\cdot 5\text{H}_2\text{O}\cdot 0.5\text{EtOH}$ complex (3), showed weight losses at temperature ranges 25-135 °C and 137-175 °C due to removal of 0.5 ethanol molecule and five water molecules, respectively. The thermal decomposition begins at 175 °C via a progressive stage associated by 55.97% weight loss. This step is characterized by a sharp DTG peak at $T_{\text{max.}}=236$ °C and corresponding to ligand pyrolysis ($2\text{C}_{12}\text{H}_{13}\text{N}_4\text{OS}$). The decomposition is continued within the temperature range 390-1000 °C with weight loss equivalent to removal of $\text{C}_{13}\text{H}_{10}\text{N}_2\text{O}$. The

thermogram of $[\text{Ni}(\text{HL})\text{Cl}]\cdot 2.5\text{H}_2\text{O}\cdot 0.25\text{EtOH}$ (4), $[\text{Cu}(\text{HL})\text{Cl}]\cdot 3.75\text{H}_2\text{O}$ (6) and $[\text{Cu}(\text{HL})(\text{CH}_3\text{COO})]\cdot 2.25\text{H}_2\text{O}$ (7) complexes establish that they are isothermal for all the three complexes. The dehydration and/desolvation processes occur within range 25-250 °C. The thermal decomposition stage associated with 41.63, 41.32 and 44.92% TG weight losses at (210-450), (250-400) and (200-410 °C) regions for (4), (6) and (7) respectively. The TG weight losses are compatible with removal of $(\text{C}_{11}\text{H}_{11}\text{N}_2\text{O})$ fragment along with elimination of anions. Also, the weight loss is continued in the range 450-1000 °C leaving metal oxide and variable amount of organic residue.

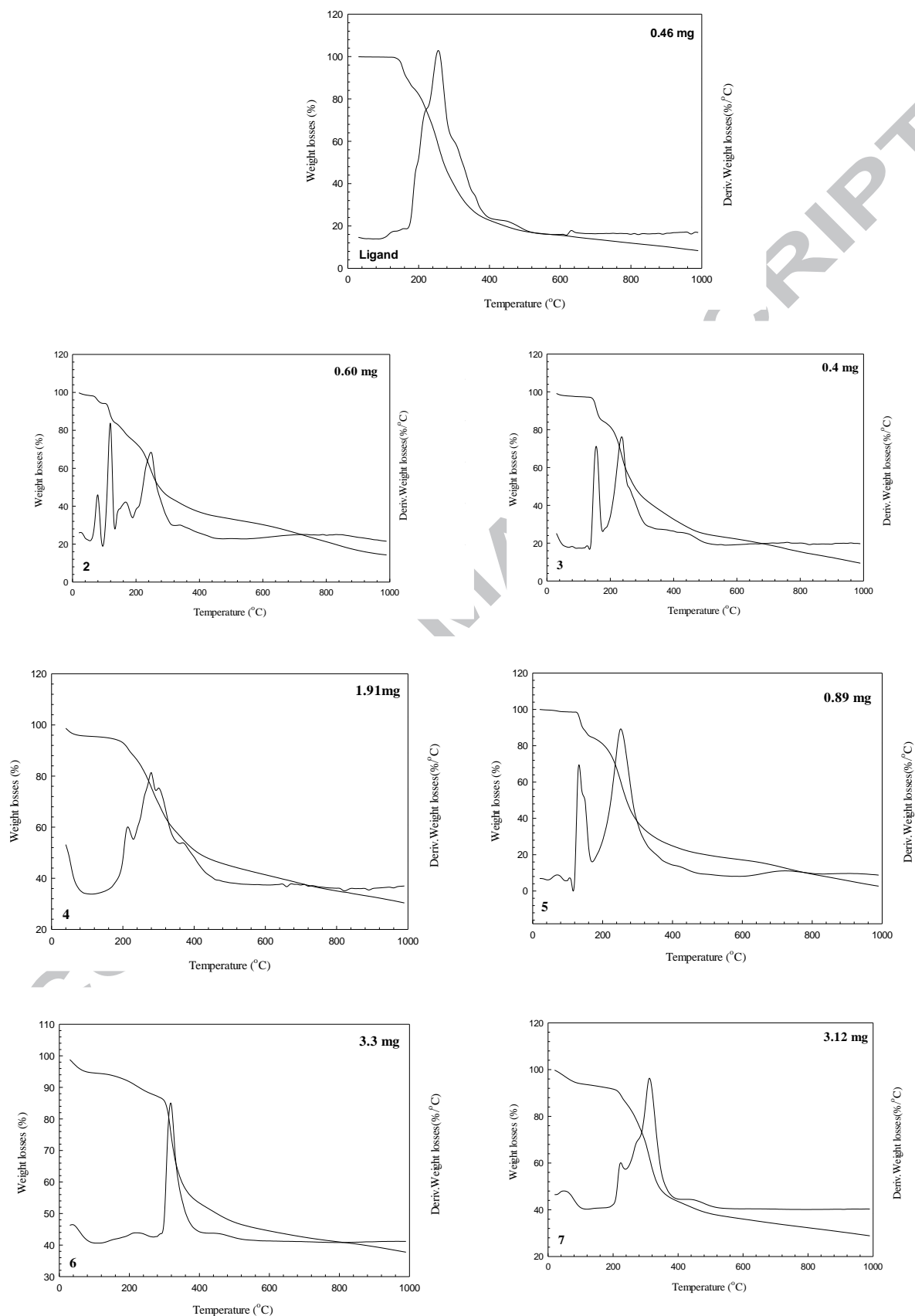
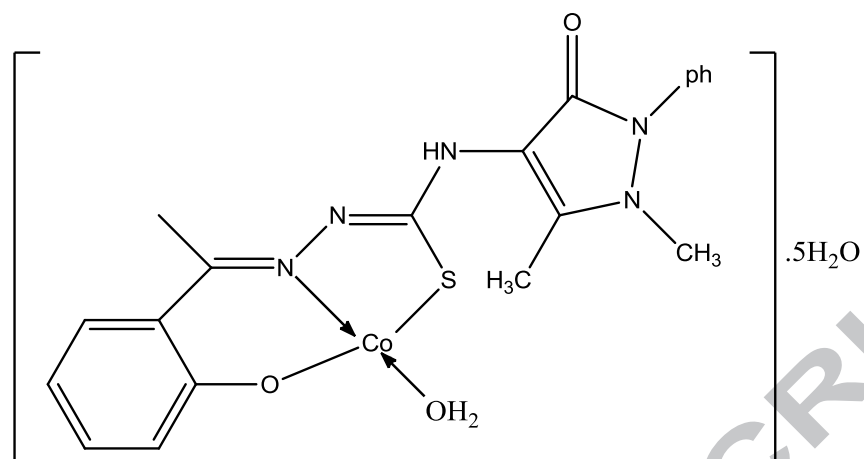


Fig. 5 Thermograms of ligand and its metal complexes (1-6)

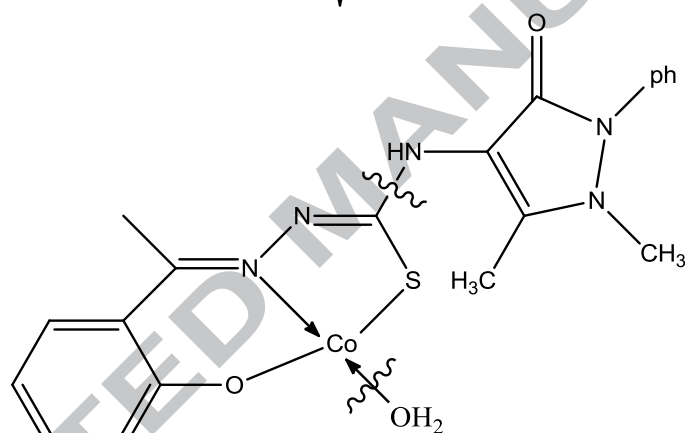
Table 6 Thermal decomposition of the ligand and its metal complexes

No.	Compound	TG range (°C)	DTG peak (°C)	Mass Loss %		Assignments*
				Found	Calcd.	
	H ₂ L	25-155	-	-	-	-
		155-420	255	80.86	81.10	Loss of C ₁₃ H ₁₉ N ₅ O ₂ S
		420-1000		11.34	11.81	Loss of 3.75 C
		At 1000		7.69	7.08	2.25 C ^r
2	[Co(L)H ₂ O].5H ₂ O	25-140	118	16.15	16.48	Loss of 5 H ₂ O molecules ^a
		140-350	168	41.79	41.13	Loss of (H ₂ O+C ₁₁ H ₁₂ N ₃ O)
		350-1000	249	28.42	29.13	Loss of (C _{7.75} H ₅ N ₂ S)
		At 1000	770	14.20	14.26	CoO+0.25C ^r
3	[Co(HL) ₂].5H ₂ O.0.5EtOH	25-135	-	2.56	2.47	Loss of 0.5 EtOH molecule ^b
		135-175	154	10.01	9.66	Loss of 5 H ₂ O molecules ^a
		175-390	236	55.79	56.02	Loss of 2(C ₁₂ H ₁₃ N ₄ OS)
		390-1000	740	23.01	22.53	Loss of (C ₁₃ H ₁₀ N ₂ O)
		At 1000		9.26	9.32	CoO+C ^r
4	[Ni(HL)Cl].2.5H ₂ O.0.25EtOH	25-100	-	4.42	3.86	Loss of (0.25 EtOH ^b + 0.5 H ₂ O ^a)
		100-210	200	7.33	6.78	Loss of 2 H ₂ O molecules ^a
		210-500	260	41.63	41.92	Loss of (C ₁₁ H ₁₁ N ₂ O + 0.5Cl ₂)
		500-1000	680	16.32	16.78	Loss of (C _{0.75} H ₆ N ₃ S)
		At 1000		30.28	30.46	NiO+7.25C ^r
5	[Ni(L)H ₂ O].3.5H ₂ O	25-100	70	1.39	1.83	Loss of 0.5 H ₂ O molecule ^a
		100-180	150	10.91	10.41	Loss of 3 H ₂ O molecules ^a
		180-1000	253	43.05	42.42	Loss of (H ₂ O+C ₁₉ H ₁₇ N ₅ O ₂ S)
			723	28.99	28.73	Loss of (C ₇ H ₅ N ₂ S)
		At 1000		14.54	14.33	NiO ^r
6	[Cu(HL)Cl].3.75H ₂ O	25-250	220	12.33	12.35	Loss of 3.75 H ₂ O molecules ^a
		250-400	317	41.32	40.71	Loss of (C ₁₁ H ₁₁ N ₂ O + 0.5Cl ₂)
		400-1000	437	9.3	8.61	Loss of (HNS)
		At 1000		37.62	38.15	CuO+ organic residue ^r
7	[Cu(HL)(CH ₃ COO)].2.25H ₂ O	25-200	49	7.78	7.47	Loss of 2.25 H ₂ O molecule ^a
		200-400	311	63.34	63.72	Loss of acetate ion
		400-1000	429	44.92	45.31	Loss of C ₁₁ H ₁₁ N ₂ O
		At 1000		13.85	14.19	
				28.74	28.63	CuO+ organic residue ^r

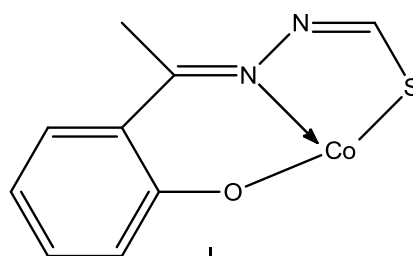
*^a dehydration, ^b desolvation and ^r final residue.



20-140 °C
- (5H₂O)



140-350 °C
- (H₂O + C₁₁H₁₂N₃O)



350-1000 °C
- (C_{7.25}H₅N₂S)

CoO + 0.25 C (14.20%)

Scheme 2. The proposed mechanism for thermal degradation of the complex [Co(L)(H₂O)].5H₂O

3.6. Electronic spin resonance (ESR) spectral studies

The ESR spectra of the solid copper(II) complexes (**6-8**) were recorded at room temperature on the X-band at frequency 9.71 GHz and the g factors were quoted relative to the standard marker DPPH ($g = 2.0037$). The ESR parameters for the polycrystalline state at 298 K are given in Table 7.

Table 7

ESR spectral parameters of the copper(II) complexes of salicylaldehyde N(4)-antipyrinylthiosemicarbazone.

Parameter	Complex (6)	Complex (7)	Complex (8)
g_{\parallel}	2.103	2.151	2.197
g_{\perp}	2.030	2.064	2.078
g_{av}^a	2.054	2.093	2.118
G	3.635	2.410	2.572
$A_{\parallel}/x 10^{-4} (cm^{-1})$			164.3
$A_{\perp}/x 10^{-4} (cm^{-1})$			48.7
Δ_2	14680	14280	16240
Δ_3	18260	17540	18600
k_{\parallel}^2	0.60	0.68	0.43
k_{\perp}^2	0.59	0.65	0.49
K	0.59	0.66	0.47
α^2			0.59
β^2			0.41
γ^2			0.74
F			129

The spectra of the complexes **6 - 8** display absorption typical for Cu(II) chelates and showed typical axial type symmetry (Fig. 7), with well-defined g_{\parallel} and g_{\perp} values [60]. In all copper(II) complexes, $g_{\parallel} > g_{\perp} > g_e$ (2.0023), indicating the unpaired electron lies predominantly in $d_{x^2-y^2}$ orbital, giving $^2B_{1g}$ as the ground state [62]. In addition, exchange coupling interaction between two Cu(II) ions is explained by Hathaway expression $G = (g_{\parallel} - 2.0023)/(g_{\perp} - 2.0023)$. When the value $G < 4.0$, a considerable exchange coupling is present in solid complexes ($G = 2.410 - 3.635$) [64]. Kivelson and Neiman showed that for an ionic environment g_{\parallel} is normally 2.3 or larger, but for covalent environment g_{\parallel} are less than 2.3 [65]. Since the g values for the complexes (Table 7) are less than 2.3, this indicates significant covalent character in the metal–ligand bonding. **The**

spectrum of complex 8 (Fig. S5), display a hyperfine spectral lines at the lower field where the values of the $g_{//}$, g_{\perp} , $A_{//}$ and A_{\perp} have been predicated (Table 7). The bonding factors α^2 , β^2 and γ^2 which can be used as a measure of the covalence of the in- plane σ bonds, in-plane and out-of-plane π - bonds respectively, have been calculated. α^2 was calculated by the following equation [60] $\alpha^2 = A_{//}/0.036 + (g_{//} - 2.0023) + 3/7(g_{\perp} - 2.0023) + 0.04$. If the value of $\alpha^2 = 0.5$, this means a complete covalent character, while a value of $\alpha^2 = 1$ proposes complete ionic bonding. The calculated value of α^2 for [Cu(HL)(ClO₄)]complex is 0.59 indicating portion of unpaired electron density sited on the Cu(II) ion. The orbital reduction factors $K_{//}$ and K_{\perp} which may be used to measure the degree of covalency of the in-plane π -bonding and out-of plane π -bonding, respectively can be calculated using the following expressions [67].

$$K_{//}^2 = (g_{//} - 2.0023)\Delta_2/8\lambda_0$$

$$K_{\perp}^2 = (g_{\perp} - 2.0023)\Delta_3/2\lambda_0$$

where λ_0 is the spin-orbit coupling of the free copper(II) ion ($\lambda_0 = -828 \text{ cm}^{-1}$)

Hathaway [68] refers that, for pure sigma bonding, $K_{//} \cong K_{\perp} \cong 0.77$ and for in-plane π -bonding, $K_{//} < K_{\perp}$; while for out-of-plane π -bonding, $K_{//} > K_{\perp}$. For [Cu(HL)Cl] and [Cu(HL)(CH₃COO)] complexes, it is observed that $K_{//} > K_{\perp}$ which shows the occurrence of significant out-of-plane π -bonding while, for [Cu(HL)(ClO₄)] complex $K_{//} < K_{\perp}$ indicating considerable in-plane π -bonding [69]. Moreover, the lower values of K than unity (0.47- 0.66) are revealing of their covalent environment [70]. In addition, the values of β^2 and γ^2 (0.41 and 0.74) for this complex indicating the presence of in-plane and out-of-plane π -bonding character for the Cu-ligand bond [71].

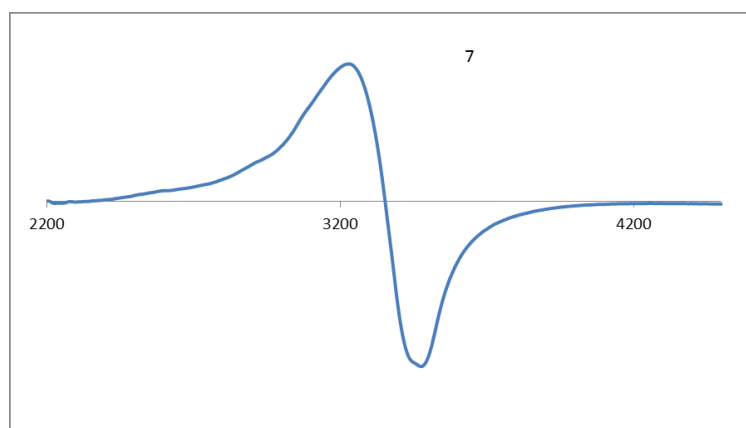


Fig. 6 ESR spectra of the solid copper(II) complexes

3.8. Biological activity

The *in vitro* antibacterial activity of the prepared ligand and its metal complexes were evaluated against the human pathogenic bacteria, Gram positive *Staphylococcus aureus* and Gram negative *Escherichia coli* using disc diffusion method. The radial growth of the colony was recorded on completion of the incubation, and the mean diameter for each compound at a concentration of 5 mg/mL was recorded. DMSO was used as a solvent and the mean inhibition zone were measured and compared with standard antibiotic, Enrofloxacin (5 mg/mL). The results are described in Table 8.

Table 8

In vitro antibacterial activity by a gar diffusion method of tested compounds

Comps.	Microorganism inhibition zone diameter (mm)	
	Gram +ve bacteria	Gram -ve bacteria
	<i>Staphylococcus aureus</i>	<i>Escherichia coli</i>
HL	7.4	6.2
1	7.6	7.2
2	7.4	7.8
3	7.9	7.6
4	7.9	8.4
5	7.5	8.1
6	17.8	15.9
7	17.6	10.8
8	8.0	9.5
DMSO	-	-
Enrofloxacin	26.3	-

A comparative study of the growth inhibition zone values of the organic ligand and its metal complexes are shown in diagram 1 and indicates that complexes show higher antibacterial activity as compared to the organic ligand and the zones of inhibition of all complexes were, however, lesser as compared to the standard Enrofloxacin. This is may be due the greater lipophilic nature of the complexes. Such improved activity of the complexes can be clarified on the basis of Overtone's concept and Tweedy's chelation theory [72]. According to Overtone's theory, the lipid membrane that surrounds the cell favors the passage of only lipid soluble materials owing to liposolubility is considered to be a vital factor that controls the antimicrobial activity. On chelation, the polarity of the metal ion will be reduced to a greater extent owing to the overlap of the ligand orbital and partial sharing of positive charge of metal ion with donor groups [73, 74]. Moreover, it increases the delocalization of the π electrons above the entire chelate ring and increases the lipophilicity of the complex. This increased lipophilicity increases the penetration of the complexes through lipid membrane and thus blocks the metal binding sites on enzymes of microorganisms [75]. The difference in the activity of different complexes against different organisms depend either on the impermeability of the cells of the microbes or change in ribosomes of microbial cells. The inhibition zones of antibacterial activity are presented in the Table 8. The results indicated that the ligand and its complexes did not exhibit a noticeable antibacterial activity against *Escherichia coli* except $[\text{Cu}(\text{HL})\text{Cl}]\cdot 3.75\text{H}_2\text{O}$, complex has a comparable zone of inhibition (15.9 mm) to the ligand (6.2 mm). The remarkable antibacterial results showed that the copper(II) complexes are effective potential as antibacterial agents in comparison to Schiff base and other complexes against gram positive *Staphylococcus aureus*. The similar activity of complexes 6 and 7 against *Staphylococcus aureus* appears to indicate that the nature of the counter ion ($\text{X} = \text{Cl}^-$ or OAc^- respectively) is not important. It is worth observing that the assessment of antibacterial activity of the compounds against the selected types of bacteria (Table 8) showed that $\text{Cu(II)} > \text{Ni(II)} > \text{Co(II)}$ [76].

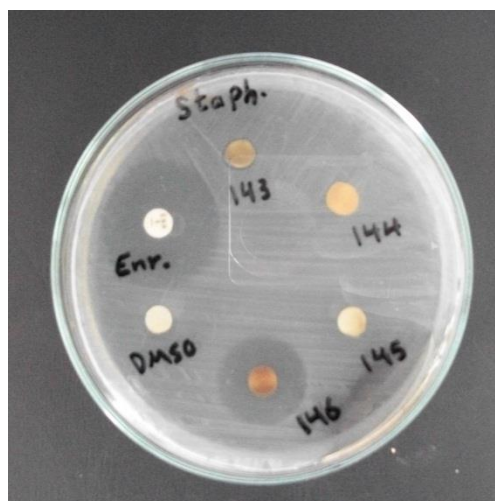
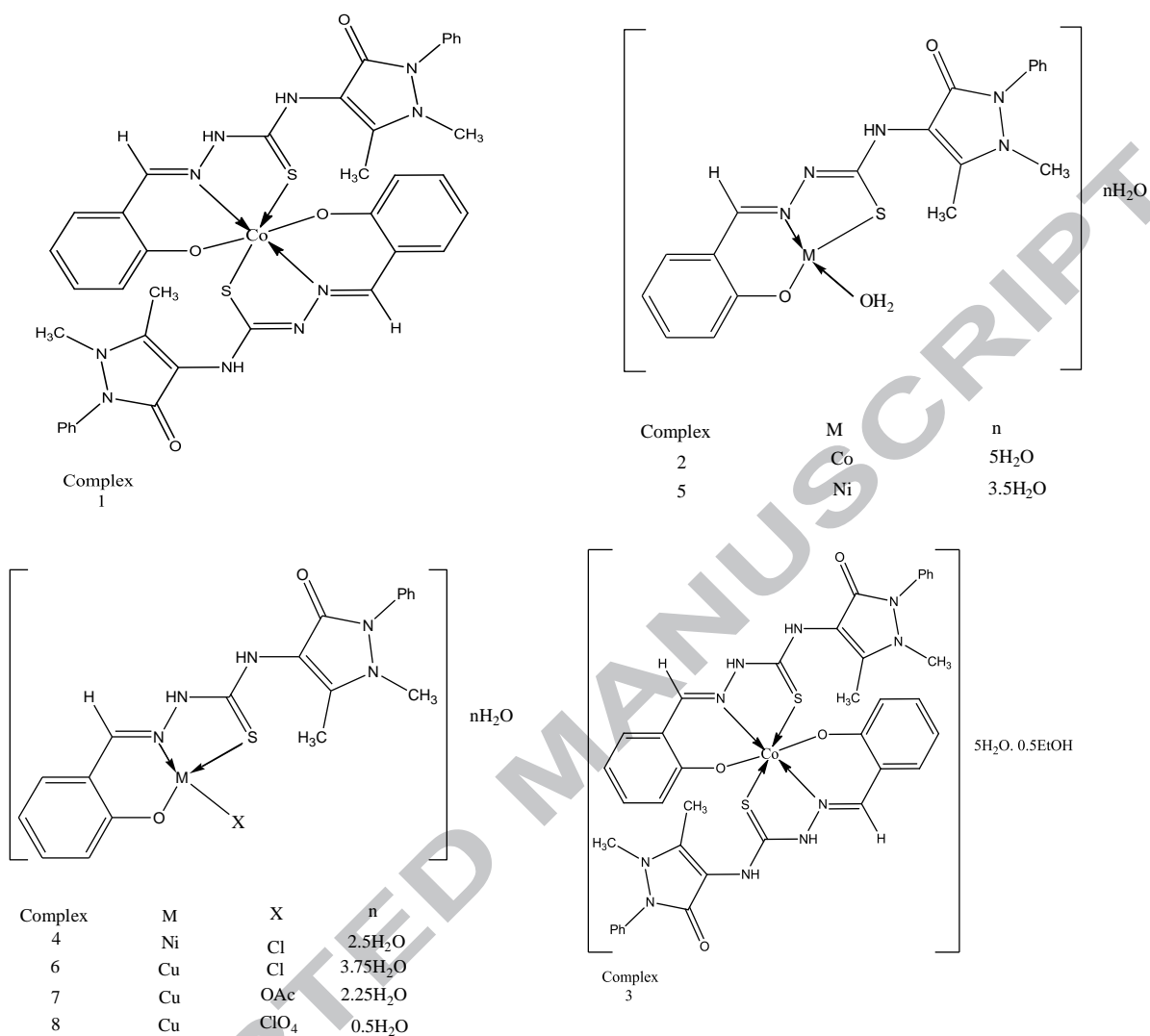


Diagram 1. The zone effect of the complexes 1, 2, 4 and 8

4. Conclusion

In this paper a new Salicylaldehyde N(4)-antipyrinythiosemicarbazone (H_2L) ligand and some of its transition metal complexes have been prepared and characterized. The elucidated 3D structure of the synthesized ligand is confirmed by comparing its experimental and predicting spectra, where the correlation are relatively good. Based on various analytical and physicochemical studies as elemental analyses, molar conductance, magnetic, thermal and spectral (1H -NMR, IR, UV-Vis, ESR) studies, a square planar or octahedral geometry may be proposed for the complexes (Scheme 3). The organic ligand may act as monobasic or dibasic tridentate coordinating to the metal ion through ONS. The antibacterial studies of the prepared compounds screened against pathogenic bacteria indicates that copper(II) complexes have higher activities than the free thiosemicarbazone and all other complexes.



Scheme 3. The proposed Structures for metal complexes.

References

- [1] D. Mishra, S. Naskar, M.G. Drew, S.K. Chattopadhyay, *Inorganica Chim. Acta* 359 (2006) 585-592.
- [2] J. Casas, M. Garcia-Tasende, J. Sordo, *Coord. Chem. Rev.* 209 (2000) 197-261.
- [3] S.D. Khanye, B. Wan, S.G. Franzblau, J. Gut, P.J. Rosenthal, G.S. Smith, K. Chibale, J. *Organomet. Chem.* 696 (2011) 3392-3396.
- [4] D. Kovala-Demertzi, A. Boccarelli, M. Demertzis, M. Coluccia, *Chemotherapy* 53 (2007) 148-152.
- [5] M. Khandani, T. Sedaghat, N. Erfani, M.R. Haghshenas, H.R. Khavasi, *J. Mol. Str.* 1037 (2013) 136-143.
- [6] K. Singh, J.P. Tandon, *Monatsh. Chem.* 123 (1992) 315-319.
- [7] A. Syamal, S. Ahmed, M.B. Niazi, *Indian J. Chem. Soc.* 60 (1983) 493-495.
- [8] T.S. Lobana, R. Sharma, G. Bawa, S. Khanna, *Coord. Chem. Rev.* 253 (2009) 977-1055.
- [9] F.R. Pavan, P.I.d.S. Maia, S.R.A. Leite, V.M. Deflon, A.A. Batista, D.N. Sato, S.G. Franzblau, C.Q.F. Leite, *Eur. J. Med. Chem.* 45 (2010) 1898-1905.
- [10] M.C. Rodríguez-Argüelles, P. Tourón-Touceda, R. Cao, A.M. García-Deibe, P. Pelagatti, C. Pelizzi, F. Zani, *J. Inorg. Biochem.* 103 (2009) 35-42.
- [11] P. Bindu, M.R.P. Kurup, T.R. Satyakeerty, *Polyhedron* 18 (1998) 321-331.
- [12] N.S. Youssef, A.M.A. El-Seidy, M. Schiavoni, B. Castano, F. Ragaini, E. Gallo, A. Caselli, J. *Organomet. Chem.* 714 (2012) 94-103.
- [13] A.H. Pathan, R.P. Bakale, G.N. Naik, C.S. Frampton, K.B. Gudasi, *Polyhedron* 34 (2012) 149-156.
- [14] A.K. El-Sawaf, D.X. West, F.A. El-Saied, R.M. El-Bahnasawy, *Transit. Metal Chem.* 23 (1998) 565-572.
- [15] A.K. El-Sawaf, D.X. West, F.A. El-Saied, R.M. El-Bahnasawy, *Transit. Metal Chem.* 23 (1998) 649-655.
- [16] A.K. El-Sawaf, F. El-Essawy, A.A. Nassar, E.-S.A. El-Samanody, *J. Mol. Str.* 1157 (2018) 381-394.
- [17] T.S. Lobana, S. Indoria, A.K. Jassal, H. Kaur, D.S. Arora, J.P. Jasinski, *Eur. J. Med. Chem.* 76 (2014) 145-154.
- [18] A.D. Becke, *J. Chem. Phys.* 98 (1993) 5648-52.
- [19] M. Andersson, P. Uvdal, *J. Phys. Chem. A* 109 (2005) 2937-2941.
- [20] F. Furche, R. Ahlrichs, *J. Chem. Phys.* 117 (2002) 7433.

- [21] G. Scalmani, M.J. Frisch, B. Mennucci, J. Tomasi, R. Cammi, V. Barone, T J. Chem. Phys. 124 (2006) 094107.
- [22] J. Gauss, J. Chem. Phys. 99 (1993) 3629-43.
- [23] J. Tomasi, B. Mennucci, R. Cammi, Chem. Rev. 105 (2005) 2999-3093.
- [24] D. Jacquemin, V. Wathelet, E.A. Perpète, C. Adamo, J. Chem. Theory Comput. 5 (2009) 2420-2435.
- [25] M. J. Frisch, G. W. Trucks, H. B. Schlegel, G. E. Scuseria, M. A. Robb, J. R. Cheeseman, G. Scalmani, V. Barone, B. Mennucci, G. A. Petersson, H. Nakatsuji, M. Caricato, X. Li, H. P. Hratchian, A. F. Izmaylov, J. Bloino, G. Zheng, J. L. Sonnenberg, M. Hada, M. Ehara, K. , R. F. Toyota, J. Hasegawa, M. Ishida, T. Nakajima, Y. Honda, O. Kitao, H. Nakai, T. Vreven, J. A. Montgomery, Jr., J. E. Peralta, F. Ogliaro, M. Bearpark, J. J. Heyd, E. Brothers, K. N. Kudin, V. N. Staroverov, R. Kobayashi, J. Normand, K. Raghavachari, A. Rendell, J. C., S. S. I. Burant, J. Tomasi, M. Cossi, N. Rega, J. M. Millam, M. Klene, J. E. Knox, J. B. Cross, V. Bakken, C. Adamo, J. Jaramillo, R. Gomperts, R. E. Stratmann, O. Yazyev, A. J. Austin, R. Cammi, C. Pomelli, J. W. Ochterski, R. L. Martin, K. Morokuma, V. G. Zakrzewski, P. S. G. A. Voth, J. J. Dannenberg, S. Dapprich, A. D. Daniels, O. Farkas, J. B. Foresman and J. C. J. V. Ortiz, and D. J. Fox, *Gaussian 09, Revision A.02*, 2009.
- [26] A. Bauer, W. Kirby, J.C. Sherris, M. Turck, Am. J. Clin. Pathol. 45 (1966) 493.
- [27] S.S. Konstantinović, B.C. Radovanović, A. Krklješ, J. Therm. Anal. Calorim. 90 (2007) 525-531.
- [28] S.A. Patil, V.H. Naik, A.D. Kulkarni, P.S. Badami, Spectrochim. Acta A 75 (2010) 347-354.
- [29] S. Anitha, J. Karthikeyan, A.N. Shetty, J. Struct. Chem. 53 (2012) 932-937.
- [30] R. Dinda, C.S. Schmiesing, E. Sinn, Y.P. Patil, M. Nethaji, H. Stoeckli-Evans, R. Acharyya, Polyhedron 50 (2013) 354-363.
- [31] S. Naskar, D. Mishra, R.J. Butcher, S.K. Chattopadhyay, Polyhedron 26 (2007) 3703-3714.
- [32] D. X. West, B. L. Mokijewski, H. Gebremedhin and T. J. Romack, Transition Met. Chem. 17 (1992) 384-386.
- [33] A. Castineiras, D. X. West, H. Gebremedhin and T. J. Romack, Inorg. Chim. Acta 216 (1994) 229-236.
- [34] R. Carballo, A. Castineiras, T. Perez, Z. Naturforsch. B Chem. Sci. 56 (2001) 881-888.
- [35] A. Gulea, D. Poirier, J. Roy, V. Stavila, I. Bulimestru, V. Tapcov, M. Birca, L. Popovschi, J. Enzyme Inhib. Med. Chem. 23 (2008) 806-818.
- [36] L. Larabi, Y. Harek, A. Reguig, M. Mostafa, J. Serb. Chem. Soc. 68 (2003) 85-96.

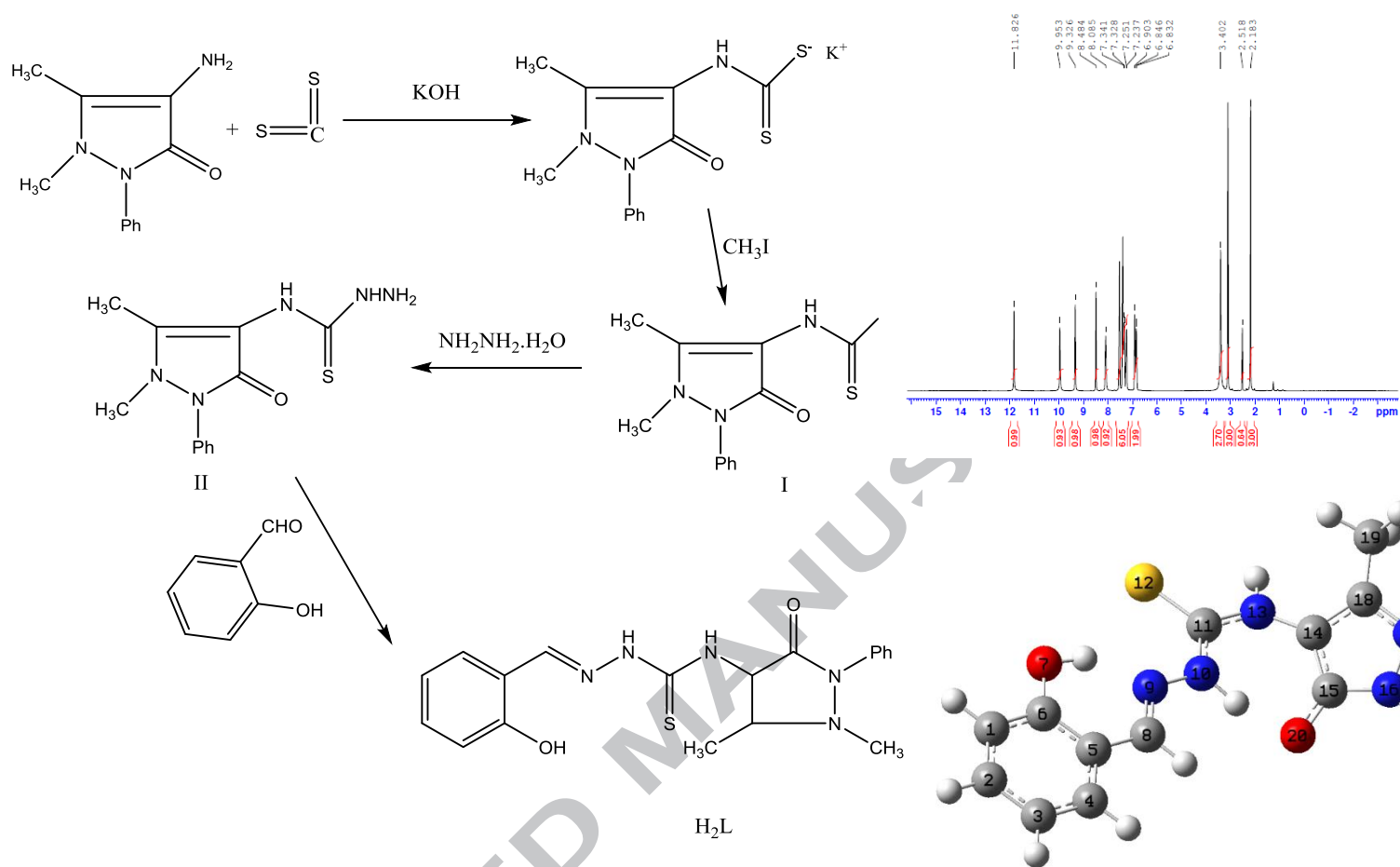
- [37] M.J. Campbell, *Coord. Chem. Rev.* 15 (1975) 279-319.
- [38] O.E. Offiong, *Transit. Metal Chem.* 20 (1995) 126-131.
- [39] K. Shah, K. Shah, *J. Indian Chem. Soc.* 62 (1985) 729-730.
- [40] N.T. Akinchan, D.X. West, Y.H. Yang, M.M. Salberg, T.L. Klein, *Transit. Metal Chem.* 20 (1995) 481-484.
- [41] M.A. Ali, R. Bose, *J. Inorg. Nucl. Chem.* 39 (1977) 265-269.
- [42] C.M. Abu El-Reash, M.M. Bekheit, M.E. Khalifa, K.M. Ibrahim, *Synth. React. Inorg. Met. Org. Chem.* 18 (1988) 1023-1038.
- [43] D.X. West, S.B. Padhye, P.B. Sonawane, *Structural and physical correlations in the biological properties of transition metal heterocyclic thiosemicarbazone and S-alkyldithiocarbazate complexes*, *Complex Chemistry*, Springer 1991, pp. 1-50.
- [44] D.X. West, L.K. Pannell, *Transit. Metal Chem.* 14 (1989) 457-462.
- [45] M. Teotia, J. Gurtu, V. Rana, *J. Inorg. Nucl. Chem.* 42 (1980) 821-831.
- [46] A. El-Dissouky, A. Fahmy, A. Amer, *Inorganica Chim. Acta* 133 (1987) 311-316.
- [47] G. Deacon, R. Phillips, *Coord. Chem. Rev.* 33 (1980) 227-250.
- [48] N.S. Youssef, K. Hegab, *Synth. React. Inorg. Met. Org. Chem.* 35 (2005) 391-399.
- [49] V. Gayathri, N. Shashikala, N. Gowda, G. Reddy, *Ind. J. Chem.* 32 (1993) 6.
- [50] V. Philip, V. Suni, M.R.P. Kurup, M. Nethaji, *Polyhedron* 25 (2006) 1931-1938.
- [51] D.X. West, M.M. Salberg, G.A. Bain, A.E. Liberta, *Transit. Metal Chem.* 22 (1997) 180-184.
- [52] E.H. Anouar, J.-F.F. Weber, *Spectrochim. Acta A* 115 (2013) 675-682.
- [53] E.H. Anouar, J. Gierschner, J.-L. Duroux, P. Trouillas, *Food Chemistry* 131 (2012) 79-89.
- [54] Z.B.K.A. Trabolsy, E.H. Anouar, N.S.S. Zakaria, M. Zulkeflee, M.H. Hasan, M.M. Zin, R. Ahmad, S. Sultan, J.-F.F. Weber, *J. Mol. Str.* 1060 (2014) 102-110.
- [55] E.W. Ainscough, A.M. Brodie, N.G. Larsen, *Inorg. Chim. Acta* 60 (1982) 25-34.
- [56] D.J. Radanović, M.I. Djuran, T.S. Kostić, C. Maricondi, B.E. Douglas, *Inorganica Chim. Acta* 207 (1993) 111-119.
- [57] S.A. El-Fetoh, A. Eid, A.A. El-Kareem, M. Wassel, *Synth. React. Inorg. Met. Org. Chem.* 30 (2000) 513-532.
- [58] H.F.A. El-halim, M. Omar, G.G. Mohamed, *Spectrochim. Acta A* 78 (2011) 36-44.
- [59] A. El-Asmy, K. Ibrahim, M. Bekheit, M. Mostafa, *Synth. React. Inorg. Met. Org. Chem.* 15 (1985) 287-300.
- [60] S. Chandra, M. Tyagi, K. Sharma, *J. Iran Chem. Soc.* 6 (2009) 310-316.
- [61] A. Prakash, M.P. Gangwar, K. Singh, *J. Dev. Biol. Tissue Eng.* 3 (2011) 13-19.

- [62] K.B. Gudasi, S.A. Patil, R.S. Vadavi, R.V. Shenoy, M. Nethaji, *Trans. Metal Chem.* 31 (2006) 586-592.
- [63] R. Roy, M. Chaudhury, S. K. Mondal and K. Nag., *J. Chem. Soc. Dalton Trans.* 0 (1984) 1681-1686.
- [64] M. Fouda, M. Abd-Elzaher, M. Shakdofa, F. El Saied, M. Ayad, A. El Tabl, *Trans. Metal Chem.* 33 (2008) 219-228.
- [65] D. Kivelson, R. Neiman, *J. Chem. Phys.* 35 (1961) 149-155.
- [66] A. H. Maki, B. R. McGarvey, *J. Chem. Phys.* 29 (1958) 35–38.
- [67] B. N. Figgis, *Introduction to Ligand Fields*, Interscience, New York, 1966.
- [68] B. J. Hathaway, *Struct. Bonding* 14 (1973) 60-pp.
- [69] W. H. Mahmoud, G. G. Mohamed, M. M. I El-Dessouky, *Spectrochim. Acta A* 122 (2014) 598–608.
- [70] H. A. EL-Boraey, S. M. Emam, D. A. Tolan, A. M. El-Nahas, *Spectrochim. Acta A.* 78 (2011) 360–70.
- [71] P. J. Rohith, A. Sreekanth, V. Rajakannan, T.A. Ajith, M.R. Prathapachandra Kurup, *Polyhedron* 23 (2004) 2549–2559.
- [72] B. Tweedy, *Phytopathology* 55 (1964) 910-914.
- [73] K. Kráľová, K. Kissova, O. Švajlenová, J. Vančo, *Chem. Pap* 58 (2004) 357-361.
- [74] J. Parekh, P. Inamdhar, R. Nair, S. Baluja, S. Chanda, *J. Serb. Chem. Soc.* 70 (2005) 1155-1162.
- [75] Y.K. Vaghasiya, R. Nair, M. Soni, S. Baluja, S. Shanda, *J. Serb. Chem. Soc.* 69 (2004) 991-998.
- [76] M.C. Rodríguez-Argüelles, A. Sánchez, M.B. Ferrari, G.G. Fava, C. Pelizzi, G. Pelosi, R. Albertini, P. Lunghi, S. Pinelli, *J. Inorg. Biochem.* 73 (1999) 7-15.

Highlights

- Synthesis of metal complexes with Salicylaldehyde N(4)-antipyrinylthiosemicarbazone.
- Complexes structures were characterized using spectroscopic techniques.
- DFT calculations at B3LYP allow a better reproduction of the spectroscopic data.
- Antibacterial activity against *Staphylococcus aureus* and *Escherichia coli* is investigated.

ACCEPTED MANUSCRIPT



Synthesis steps of N(4)-antipyrinylthiosemicarbazide I
 its ¹H-NMR spectrum

ACCEPTED MANUSCRIPT